Spray and Combustion Characteristics of a Dump-type Ramjet Combustor

Choong-Won Lee, Su-Yeon Moon*, Chang-Hyun Sohn
Department of Mechanical Engineering, Kyungpook National University, 1370 Sankyuk-Dong, Puk-ku, Taegu 702-701, Korea
Hyun-Jin Youn
Graduate School, Department of Mechanical Engineering, Kyungpook National University, 1370 Sankyuk-Dong, Puk-ku, Taegu 702-701, Korea

Spray and combustion characteristics of a dump-type ram-combustor equipped with a V-gutter flame holder were experimentally investigated. Spray penetrations with a change in airstream velocity, air stream temperature, and dynamic pressure ratio were measured to clarify the spray characteristics of a liquid jet injected into the subsonic vitiated airstream, which maintains a highly uniform velocity and temperature. An empirical equation was modified from Inamura's equation to compensate for experimental conditions. In the case of insufficient penetration, the flame in the ram-combustor was unstable, and vice versus in the case of sufficient penetration. When the flame holder was not equipped, the temperature at the center of the ram-combustor had a tendency to decrease due to the low penetration and insufficient mixing. Therefore, the temperature distribution was slanted to the low wall of the ram-combustor. These trends gradually disappeared as the length of the combustor became longer and the flame holder was equipped. Combustion efficiency increased when the length of the combustor was long and the flame holder was equipped. Especially, the effect of the flame holder was more dominant than that of the combustor length in light of combustion efficiency.

Key Words : Liquid-Fueled Ramjet Engine, Dump-Type Ram-Combustor, Vitiated Air Heater, Jet Penetration, Combustion Efficiency, V-gutter Flame Holder, Flame Stability

Nomenclature

AR : Aspect ratio of V-gutter
D_i : Diameter of combustor inlet (mm)
D_j : Diameter of injector tip (mm)
D_o : Diameter of combustor outlet (mm)
D_V : Height of V-gutter (mm)
h : Penetration of liquid jet in the Y direction (mm)
L_C : Length of combustor (mm)
m_a : Air mass flow rate (kg/s)
m_f : Fuel mass flow rate (kg. /s)
m_{H2} : H_2 mass flow rate (kg/s)
m_{O2} : O_2 mass flow rate (kg/s)
T_{ad} : Adiabatic flame temperature (K)
T_0 : Temperature of air at the inlet of VAH (K)
T_{exp} : Measured temperature of combustor (K)
U_a : Velocity of air at the inlet of combustor (m/s)
U_i : Velocity of air at the inlet of VAH (m/s)
U_j : Velocity of fuel jet (m/s)
X : Horizontal distance from the center of an injector exit (mm)
Y : Vertical distance from an injector exit (mm)
Z : Distance in the direction perpendicular to X and Z axis (mm)

* Corresponding Author,
E-mail : symoon@knu.ac.kr
TEL : +82-53-950-7313; **FAX** : +82-53-956-9914
Department of Mechanical Engineering, Kyungpook National University, 1370 Sankyuk-Dong, Puk-ku, Taegu 702-701, Korea. (Manuscript **Received** August 26, 2002; **Revised** September 18, 2003)

α : Wedge half angle of V-gutter (degree)
ρ_a : Density of air (kg/m^3)
ρ_j : Density of fuel (kg/m^3)
Φ : Equivalence ratio

1. Introduction

A ramjet engine, one of the simplest rocket systems, directly induces air (oxygen of propulsion system) from the atmosphere without a compression system. The induced air goes in a compression process in through a supersonic diffuser. Therefore, the ramjet engine has many advantages, such as the maximum energy transfer rate, reduction of the weight and volume, and an increase of the flight ranges.

Storable liquid fuel was attractive for use in the limited space of the ramjet engine due to its high density and heating value Waltrup (1987). However, insufficient mixing of fuel and air causes unstable combustion. Thus, spray mechanisms were carefully investigated to yield a stable flame and high combustion efficiency. The mean droplet diameters of a traverse fuel into a supersonic airstream were investigated by Nejad and Schetz (1983). An empirical equation for the penetration of a liquid jet in a subsonic airstream was deduced by Shetz and Padhye (1977) based on their measurements of the liquid jet. An empirical equation for the penetration and mean droplet diameter in a subsonic airstream was deduced by Kashiwagi (1991). Droplet mass flux and velocity distributions were studied by Inamura and Nagai (1997). However, their reports were conducted under a cold flow condition. In the actual ramjet engine, the temperature of the air induced into the combustor is higher than 500 K. Therefore, there is a need to clarify influences of hot airstream on spray characteristics.

Combustion characteristics of the liquid jet have been reported by many researchers. The relations between configurations of the fuel injector and combustion performance were elucidated by Sjoblom (1989). Vinogradov et al. (1995) investigated the combustion performance when fuel is injected parallel to the supersonic airstream in a scramjet combustor. However, the combustion characteristics in a ram-combustor equipped with flame holder have not been investigated.

Therefore, the purpose of this study is to clarify the spray mechanism and combustion characteristics in the ram-combustor with a flame holder. The penetrations in a hot air stream were measured with a change in a dynamic pressure ratio, inlet temperature, and air velocity. The temperature distributions were measured in the ram-combustor equipped with flame holder. The flame stability region and combustion efficiency were also investigated.

2. Experimental Apparatus and Conditions

A schematic diagram of an experimental apparatus is shown in Fig. 1. The experimental facilities consist of the supply section, the Vitiated Air Heater (VAH), the dump-type ram-combustor, and the measurement section. The supply section provides air and fuel (kerosene). The VAH produces the same air conditions as real-flight conditions. In the measurement section, the experimental data are recorded, using the computer and A/D converter.

Figure 2 is a detailed drawing of the VAH. The VAH directly heats up air by hydrogen-oxygen combustion. H_2 is used as the fuel and O_2 as the oxidizer in the VAH. The high velocity air and hydrogen (H_2) are mixed with a sufficient oxygen (make-up oxygen) to yield stoichiometric com bustion in the VAH. The amount of the make-up

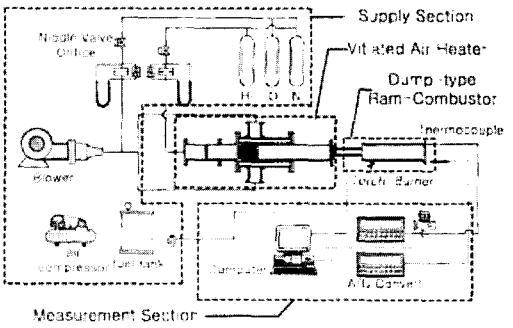

Fig. 1 Schematic diagram of experimental apparatus.

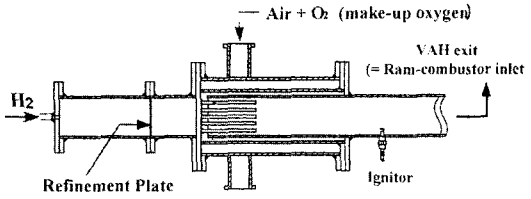

Fig. 2 Details of VAH(Vitiated Air Heater)

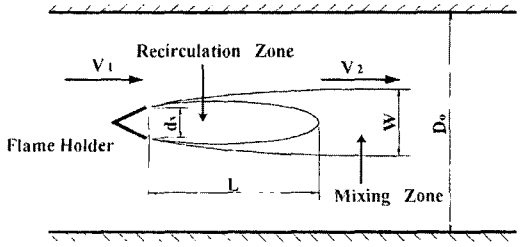

Fig. 3 Typical flame holder used in the analysis of stabilization

oxygen can be obtained by equating the mole fraction of the oxygen in the combustion products to that in atmospheric air (0.2095) AGARD (1994).

Figure 3 shows the stabilization mechanism of the bluff body flame. A V-gutter flame holder is used to stabilize the flame. Its advantages are low flow blockage and low pressure loss Mattingly (1987). The V-gutter flame holder has been designed using experimental data such as residence time and flame stabilization theory according to blockage ratio Oates (1978). The wakes of the flame holder are divided into two regions: a recirculation zone and a mixing zone. The recirculation zone is characterized by a strongly recirculating flow and low reaction rate, while the mixing zone by the formation of turbulent flows due to strong shears, steep temperature gradients, and a vigorous chemical reaction. A stable flame is established in the mixing zone by the balance of the heat and mass transfer between the cool unburned gas and the hot burned gas.

Figure 4 shows coordinate systems employed in this study. The X', Y', Z' and the X, Y, Z coordinate systems are used for measuring the velocity, temperature, oxygen volume ratio in VAH and penetration of spray at a nozzle.

The experimental conditions are shown in Table 1. It is realized from Table 1 that parameters are the length of combustor and mass flow rate of fuel.

Table 1 Experimental Conditions

VAH	Mass flow-rate of air(m_a) = 0.238 kg/s Temperature of inlet air(T_0) = 500 K Velocity of inlet air(U_1) = 120 m/s
Ram-combustor	Dia. of combustor inlet(D_i) = 50 mm Dia. of combustor outlet(D_0) = 100 mm Length of combustor(L_C) = 300 mm, 450 mm
Fuel Injector	Mass flow-rate of fuel(m_f) = 2.6, 3.9, 5.2 g/s Dia. of injector tip(D_j) = 0.92 mm
V-gutter Flame Holder	Wedge half angle(a) = 30° Aspect Ratio(AR) = 0.125 Height of V-gutter(D_v) = 15 mm

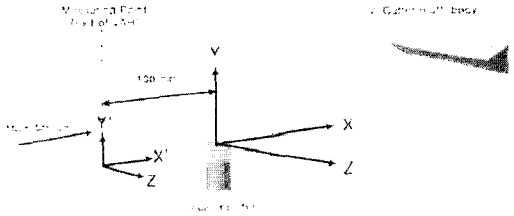

Fig. 4 Coorditate systems of measurement

3. Results and Discussions

3.1 Vitiated air heater

The temperature and velocity distributions at the exit of the VAH are represented in Fig. 5. In real-flight conditions, the temperature of the air induced into the ram-combustor rises due to the compression process of the supersonic diffuser. There is a need for an apparatus that controls the temperature and velocity of air in the ground test to satisfy the requirements of real-flight conditions. Sjoblom (1989) reported that the temperature and velocity of the real-flight conditions were a function of flight altitude and flight Mach Number. In this experiment, the flight altitude

and flight Mach number are sea level and about 3, respectirely. The temperature and velocity were determined to be 500 K and 120 m/s, according to the flight altitude and Mach number. Those values are in good agreement with the present data as shown in Fig. 5. These are uniform except that the temperature is slightly low at the wall of the VAH. Thus, it is postulated that there is no abnormal combustion in the ram-combustor due to the nonuniformity of velocity and temperature.

Figure 6 shows comparisons of the theoretical value with the experimental data of O_2 volume ratio with a variance in mass flow rates of oxygen and hydrogen. Our results are in good agreement with the theoretical values regardless of the slight changes of the mass flow rates of oxygen and hydrogen. It is noted that the accurate O_2 volume ratio could be yielded without effects of the slight changes of the amount of oxygen and hydrogen

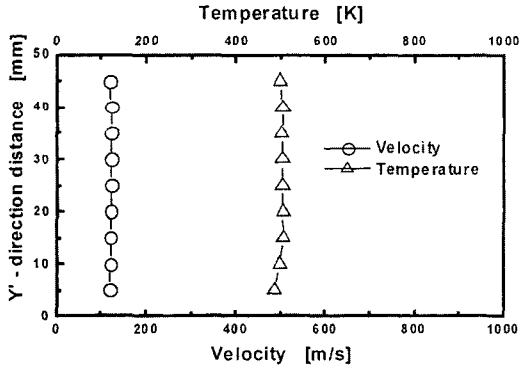

Fig. 5 Velocity and temperature distributions at the exit of the VAH

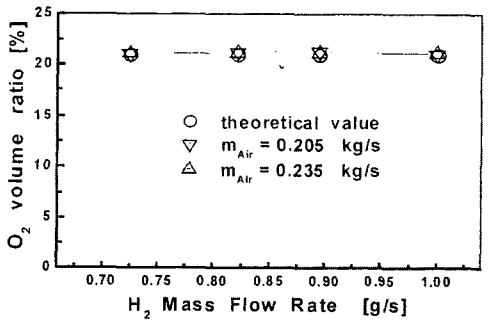

Fig. 6 Volumetric ratios of O_2 in the burned gas at the outler VAH

on the O_2 volume ratio.

3.2 Jet penetrations

Figure 7 shows characteristics of a liquid fuel jet. The liquid fuel is injected at 100 mm upstream the ram combustor. The single-orifice nozzle used in this experiment pressurizes the fuel, changes it into the liquid column and develops the liquid column into the liquid droplets. The mechanism of spray from the single-orifice nozzle is influenced by the turbulence flow, drag of the main stream, spray conditions such as density and viscosity, and aspect ratio (L_0/D_0) Bayve (1993). The jet penetration is defined as the maximum vertical distance from the outlet end of the nozzle (Y=0) to the outer visible boundary of the liquid jet at the arbitrary X point. The jet dispersion represents the vertical distance from the inner visible boundary of the jet to the outer visible boundary of the jet. Finally, the jet width can be defined as the horizontal distance from a visible boundary to the other visible boundary according to a top view Inamura (1991).

Figure 8 shows the effects of dynamic pressure ratio on jet penetration. The dynamic pressure ratio can be defined as Eq. (1)

$$q=\frac{\rho_j U_j^2}{\rho_a U_a^2} \tag{1}$$

The jet penetration increases as dynamic pressure ratios increase. As shown in Fig. 8, the jet penetration rapidly increases in the vicinity of the nozzle exit. The gradient of the penetration becomes slower due to the increase of the air-

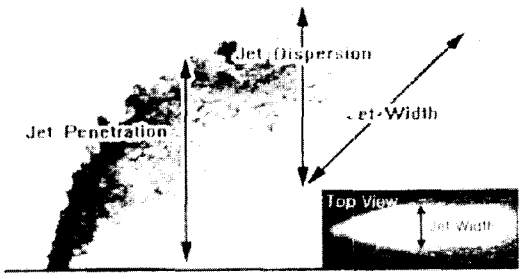

Fig. 7 Schematic instantaneous photography of a liquid jet

stream drag after the penetration jet passes $X/D_j=5$. The penetration is determined by the relative difference between the jet kinetic energy and the aerodynamic drag of the airstream. In the case of the ramjet engine, the adequate penetrations must be created since low penetrations exert bad influences on combustion performance.

Figure 9 shows the effects of airstream velocity on jet penetration. As the velocity of the airstream increases, penetration decreases due to the momentum of the airstream. Thus, the dynamic ratio becomes smaller as the velocity of the airstream increases. This results in deterioration of mixing of fuel and air.

Figure 10 indicates the effects of the airstream temperature on jet penetration. As the airstream temperature increases, jet penetration increases. This can be explained by the fact that the low density of air due to the high temperature decreases the inertia force of air. The weak inertia force of the air results in the increase of the jet penetration.

Inamura and Kashiwagi deduced the empirical equation, Eq. (2) for the jet penetration in terms of the dynamic pressure ratio Kashiwagi (1991) and Inamura et al.(1995).

$$\frac{Y}{D_0}=(1.18+0.24D_0)\left\{\frac{\rho_j U_j^2}{\rho_a U_a^2}\right\}^{0.36} \ln\left[1+(1.56+0.48D_0)\frac{X}{D_0}\right] \quad (2)$$

where D_0, X and Y represent the diameter of the combustor outlet, the distance from the nozzle exit in the direction of the airstream and the penetration length, respectively.

Figure 11 shows comparisons of experimental data with the empirical equation, Eq. (2). The experimental data are larger than the values calculated from Eq. (2). Some deviations appear due to the differences between the experimental

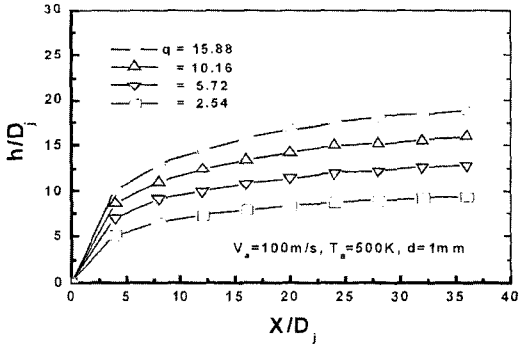

Fig. 8 Effects of dynamic ratios on jet penetrations. ($V_{air}=100$ m/s, $T_{air}=298$ K)

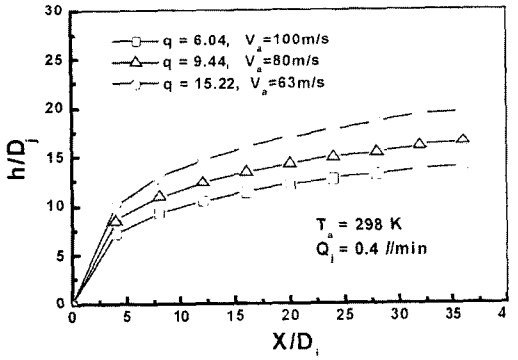

Fig. 9 Effects of air velocity on jet penetration.

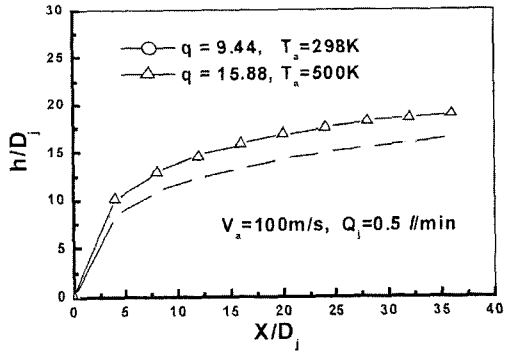

Fig. 10 Effects of air temperature on jet penetration.

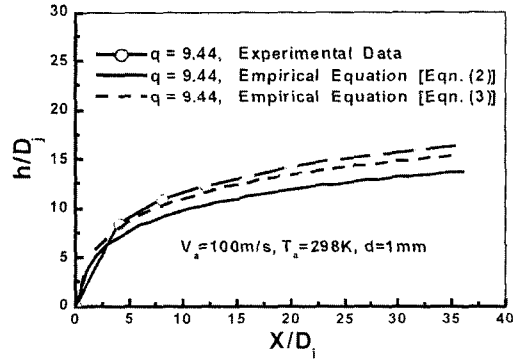

Fig. 11 Comparisons of jet penetration between measurements and calculations.

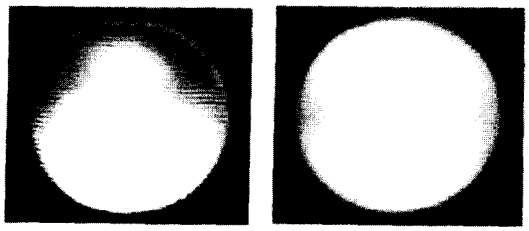

Fig. 12 Photographs of the flame with a variation in the equivalence ratio

conditions in this work and Inamula's conditions. Thus, a revised equation is suggested in Eq. (3). The revised equation is in better agreement with this experiment since the equation is deduced based on the current experimental conditions.

$$\frac{Y}{D_0}=(1.2+0.4D_0)\left\{\frac{\rho_j U_j^2}{\rho_a U_a^2}\right\}^{0.36} \ln\left[1+(1.56+0.48D_0)\frac{X}{D_0}\right] \quad (3)$$

Photographs of the flame with the variation in the equivalence ration are presented in Fig. 12. Flames are not observed around the upper section of the combustor in the case of the low equivalence ratio so that only the low section appears bright. The existence of the low regions causes a drastic change of temperature in the combustor. Complete combustion is not achieved due to the incomplete mixing in these regions. In the case of the high equivalence ratio, flames are distributed equally all around the cross section of the combustor due to the enough penetration. The results suggest that the uniformity of concentration distribution of air and fuel and flame stability are enhanced due to the extent of penetration of fuel spray.

3.3 Flame stabilization

Figure 13 shows temperature distributions at the combustor exit when the flame holder is not installed. The penetrations are not so sufficient that there are high gradients of temperature distribution at the low wall of the ram-combustor exit. In the case of the short combustor (L_C=300 mm), the temperature at the center of the combustor decreases faster due to the high velocity

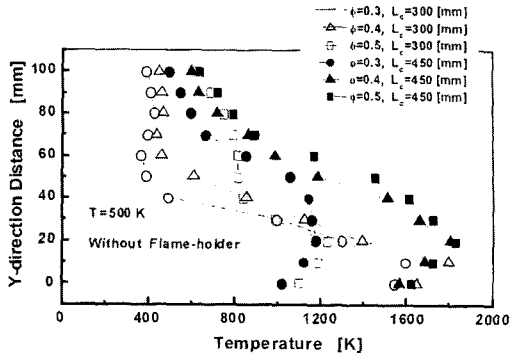

Fig. 13 Temperature profiles without V-gutter at the ram-combustor exit.

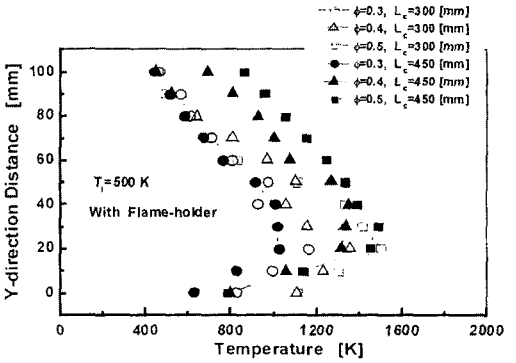

Fig. 14 Temperature profiles with V-gutter at the ram-combustor exit.

of the airstream and the insufficiency of the mixing of fuel with air. This uniformity of temperature becomes better as the equivalence ratio increases. In the long combustor (L_C=450 mm), the flame is more stable than in a short combustor (L_C=300 mm) due to the improvement of the mixing zone. The mixing performance of the fuel is improved as the length of combustor increases. Figure 14 shows the temperature distributions at the combustor exit when the flame holder is installed.

In the case of the short combustor (L_C=300 mm), the temperature still significantly changes near its low wall of the combustor because the penetration of the fuel is not sufficient. However, the effects of the recirculation zone created by the flame holder produce a more uniform temperature distribution than in the case in which the flame holder is not installed. However, the temperature

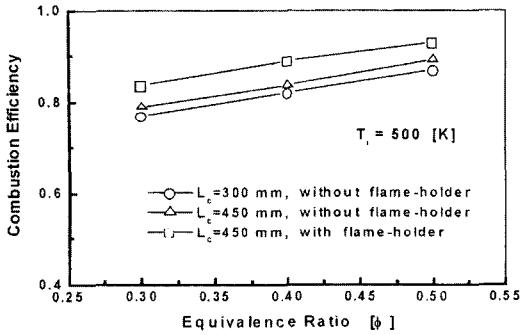

Fig. 15 Efficiencies with a variation in the equivalence ratio at the combustor exit.

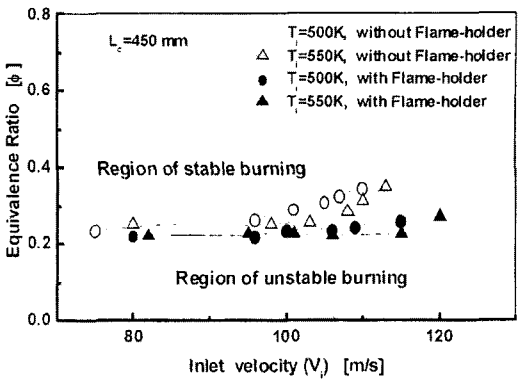

Fig. 16 Stability loop of a dump-type ram-combustor

abruptly decreases at the center of the combustor as the equivalence ratio decreases. This trend becomes less pronounced as the equivalence ratio increases and combustor length increases. The mixing performance of the fuel improves and the flame becomes more stable when the flame holder is installed and the combustor length increases.

The combustion efficiency of the combustor with a variation in the equivalent ratio is represented in Fig. 15.

$$\eta_C = \frac{\Delta T_{exp}}{\Delta T_{ad}} \tag{4}$$

The combustion efficiency is defined as Eq. (4). It can be obtained from the relation of the average exit temperature and the adiabatic flame temperature which are 1232 K and 1398 K in the condition of the mass flow rate of 0.238 kg/sec and airstream temerature of 500 K, respectively. The increases of about 5% in the combustion efficiencies are for the combustor length of 450 mm according to the existence of the flame holder. This is due to the improvement of the mixing performance caused by the flame holder. The increases of about 2% in the combustion efficiency are shown as the combustor length varies from 300 mm to 450 mm when the flame holder is not installed. This phenomenon shows that even though the flame holder has a more important influence on combustion efficiency than the variation of combustor length, it plays an important role not in the combustion efficiency but in the flame stabilization.

In Fig. 16, the lean limit of the stability loop is represented in terms of the inlet velocity and equivalence ratio. The data are arranged by the measurements of the equivalence ratio at the point of flame blow-off. Thus, the region of stable and unstable burnings can be defined as the upper and lower areas with respect to each data line. The stable region is enlarged with the increase of the airstream temperature. The result is caused by the exponential dependency of chemical reaction rates on the reaction temperature. The flame holder improves stability by extending the residence time of the reactants in the recirculation zone. Additionally, the flame stability should be simultaneously considered together with other combustor design elements such as the recoveries of pressure and the combustion efficiency.

4. Conclusions

Many performance parameters such as the jet penetration, the temperature distribution, the combustion efficiency, and the stability loop were measured to investigate the spray and combustion characteristics in a dump-type ram-combustor. Through these experiments, our conclusions can be summarized as follows:

(1) A vitiated air heater(VAH) for test facilities of ramjet engines was developed, which could satisfy a wide range of test conditions in velocity and temperature. The VAH obtained desirable velocity and temperature distributions. The compositions of vitiated air are similar to those of

real air, especially volumetric ratio of oxygen.

(2) The jet penetrations increased as the dynamic pressure ratio and air temperature increased and the velocity of the airstream decreased. The revised empirical equation was modified from Inamura's equations to compensate for our results of penetration.

(3) In the case of low penetration, there are high gradients of temperature distribution at the low wall of the ram-combustor exit. This trend become less noticeable as the flame holder is equipped. The effect of the flame holder on the flame stability is more pronounced than the increase of ram-combustor length.

(4) The combustion efficiency increased when the flame holder was installed. The flame holder had more important influence on the combustion efficiency than the variation of combustor length.

(5) The lean limit of stability loop became larger with the increase of the airstream temperature. The flame holder improved stability by extending the residence time in recirculation zone.

References

AGARD(Advisory Group for Aerospace research & Development) Advisory Report 323, 1994, pp. 51.

Bayvel L. and Orzechowski, Z., 1993, "Liquid Atomization," pp. 168.

Inamura, T., Nagai, N., Hirai, T. and Asano, H., 1991, "Disintegration Phenomena of Metalized Slurry Fuel Jets in High Speed Air Stream," Proc. 5th International Conference on Liquid Atomization and Spray System (ICLASS-91), pp. 839~846.

Inamura, T., Nagai, N., Yoshimura, K., Kumakawa, A. and Yatsuyanagi, N., 1995, "Spray Formation and Spray Combustion in Ramjet Combustor," Proc. The ASME/JSME Thermal Engineering, Honolulu, pp. 157~162.

Inamura, T. and Nagai, N., 1997, "Spray Characteristics of Liquid Jet Traversing Subsonic Airstream," Journal of Propulsion and Power, Vol. 13, No. 1.

Kashiwagi, T., 1991, "Study on afterburner of aircraft engine," Ishikawajima-Harima Engineering Review (in Japan), Vol. 31, No. 2, pp. 109~114.

Mattingly, Jack D., 1987, "Aircraft Engine Design," AIAA Education Series, pp. 324~327.

Nejad, A. S. and Schetz, J. A., 1983 "Effects of Properties and Location in the Plume on Droplet Diameter for Injection in a Supersonic Stream," AIAA Journal, Vol. 21, No. 7, pp. 956~961.

Oates, G. C., 1978, "The Aerothermodynamics of Aircraft Gas Turbine Engine," AFAPL-TR-78-52, July.

Shetz, J. A. and Padhye, A., 1977, "Penetration and Breakup of Liquids in Subsonic Airstream," AIAA Journal, Vol. 15, No. 10, pp. 1385~1390.

Sjoblom, B., 1989, "Full-Scale Liquid Fuel Ramjet Combustor Tests," ISABE, No. 89~7027, pp. 273~281.

Vinogradov, V. A., Kobigsky, S. A. and Petrov, M. D., 1995, "Experimental Investigation of Kerosene Fuel Combustion in Supersonic Flow," Journal of Propulsion and Power, Vol. 11, No. 1, pp. 130~134.

Waltrup, P. J., 1987, "Liquid-Fueled Supersonic Combustion Ramjets : A Research Perspective," Journal of Propulsion and Power, Vol. 3, pp. 515~524.